Materials Science & Engineering A 710 (2018) 385–391

Contents lists available at ScienceDirect

Materials Science & Engineering A

journal homepage: www.elsevier.com/locate/msea

Deformation induced degradation of hot-dip aluminized steel

B. Lemmens[a,b], H. Springer[c,*], M. Peeters[a], I. De Graeve[a,b], J. De Strycker[d], D. Raabe[c], K. Verbeken[a]

[a] Department Of Materials, Textiles And Chemical Engineering, Ghent University (UGent), Technologiepark 903, B-9052 Zwijnaarde, Belgium
[b] Research Group Of Electrochemical And Surface Engineering (SURF), Vrije Universiteit Brussel (VUB), Pleinlaan 2, B-1050 Brussels, Belgium
[c] Max-Planck-Institut für Eisenforschung GmbH, 40237 Düsseldorf, Germany
[d] ArcelorMittal Global R&D Gent, J.F. Kennedylaan 3, B-9060 Zelzate, Belgium

ARTICLE INFO

Keywords:
Hot-dip aluminizing
Intermetallics
Post-processing
Aluminium
Iron
Deformation

ABSTRACT

In this work the fracture and corrosion behaviour of hot-dip aluminized steels is investigated in controlled dipping experiments which allowed to separately study the effects of Si in the Al bath (1–10 wt%) and the intermetallic phase thickness (5–30 μm). The addition of Si had no direct influence on the performance of the coating system for similar thickness values of the IMP seam, which in turn showed to be the dominant factor independent from the amount of Si. Thin intermetallic phase seams (< about 10 μm) exhibited more (about 5–10 per 100 μm interfacial length) but smaller cracks with a fishnet pattern on the outer Al-Si coating, which remained intact and interconnected until a tensile deformation of 15–20%. Thicker intermetallic phase seams resulted in less (about 2 per 100 μm interfacial length) but broader cracks perpendicular to the tensile direction, giving rise to a lamellar pattern on the Al-Si coating, which cracks and uncovers the steel already at strains below 10%, and readily flakes off leaving the steel substrate to accelerated corrosion in chloride environments. Our results indicate that the reduction of the intermetallic phase seam thickness remains the main target to improve the performance of hot-dip aluminized coated steel by combining appropriate Si additions with minimized dipping temperatures and times.

1. Introduction

Steel is the most widely used construction material due to the unique combination of wide accessible ranges of mechanical properties at comparatively low cost, and thus the backbone of modern infrastructure and transportation. Among the biggest challenge in applying steels is their susceptibility to corrosion, an electrochemical process which originates at the surface of a material. Of the multitude of possible methods of corrosion protection, metallic coatings are most widely used, with aluminium (Al) increasingly replacing zinc as a coating material. Hot-dip aluminizing (HDA), i.e. dipping the steel substrate into liquid Al, is the most versatile and economic coating technique, and therefore extensively used for sheet material for automotive applications. HDA steel sheets are typically deep drawn into fuel filters and fuel tanks, as well as other parts and components where the excellent corrosion resistance of Al especially at elevated temperatures is of key importance, such as exhaust systems and heat shields [1]. The most important industrial sheet forming processes are deep drawing and stretching, where the metal sheet is formed into the desired shape by pressing it into a die. One specific type of drawing process is the hot stamping of steel sheet with or without cold pre-deformation (also called press hardening) for the production of ultra-high strength chassis components, such as the A- and B-pillar, front and rear rail, bumper and tunnel [2–6]. In order to fulfil its protective role in such (not only automotive) components, though, it is of critical importance that the HDA coating is not damaged during such forming operations, as its removal or damage potentially renders the steel substrate prone to oxidation and decarburisation at high temperatures (i.e. during the hot stamping process) and / or corrosion (i.e. rust formation) at low temperatures.

It is well known that the mechanical performance of HDA steel, and thus its corrosion protection ability, is drastically influenced by the brittle intermetallic phases (IMPs) formed due to the interdiffusion of Al and Fe during the dipping process. In order to decrease the thickness of this IMP seam between the steel substrate and Al coating, silicon (Si) is added to the Al bath [7]. The formability of such HDA steel sheets has been investigated by deep drawing [8,9] or push-out tests [10], while others used bending and tensile tests to evaluate the performance of Al-Si coated steel. Shady et al. [11] demonstrated that raising the Si content in Al increased the number of bends until peeling and flaking of the coating occurred in line with other works [12–17], and concluded

* Corresponding author.
E-mail address: h.springer@mpie.de (H. Springer).

https://doi.org/10.1016/j.msea.2017.10.094
Received 11 July 2017; Received in revised form 25 October 2017; Accepted 26 October 2017
Available online 27 October 2017
0921-5093/ © 2017 Elsevier B.V. All rights reserved.

Ex. 2018
IPR2024-01376

that the coating's performance is mainly governed by the thickness of the IMP layer.

However, Si has a more complex role and will induce several microstructural changes in HDA steel apart from the already mentioned reduction of the IMP thickness for similar processing conditions, namely, the formation of deviating types of IMPs formed at the interface with different mechanical characteristics [18], and increased strength and reduced ductility of the Al based coating [19]. Together they determine the overall performance of the coated steel in a partially contradicting manner: while increasing the Si concentration may lead to thinner IMP seams it also embrittles the overlaying Al coating. In all previous studies, though, these effects were investigated simultaneously, as they are mutually linked when identical coating parameters (e.g. dipping time and temperature) are applied. Furthermore, only little information exists on the micromechanical mechanisms of the associated failure processes [20].

In order to further improve coating compositions and parameters by deepening the understanding of the underlying phenomena, the experimental conditions in this work were chosen to study the effects of (i) IMP thickness and (ii) the role of the Si content separately, in order to evaluate their respective contributions to the overall performance of HDA steel. Firstly, IMP seams of similar thickness but stemming from experiments with different Si content were investigated. Secondly, the influence of the thickness of the IMP layers is examined while keeping the Si content unchanged but varying the dipping time. These experiments allow elucidating how Si influences the fracture behaviour of HDA coating on steel. Designated tensile samples were used to investigate the protective performance of the different coatings as a function of pre-deformation using corrosion testing. Moreover, the failure initiation and propagation is investigated in order to derive guidelines for the design and adaptation of HDA parameters.

2. Materials and methods

The hot-dip experiments were performed with a Rhesca hot-dip simulator 200-A. Steel substrates with a thickness of 0.9 mm of DC06 European grade, cut to plates of 100 mm by 200 mm, were dipped in Al baths containing 1, 5 and 10 wt% Si, respectively, at a temperature of 685 °C under a protective atmosphere of N_2 – 5% H_2 preventing the steel from oxidizing. Dipping times of 3, 60 and 300 s were applied. The thicknesses of both Al coating and IMP seam was measured by image analysis (ImageJ software) on SEM images (FEG-SEM Quanta-450). The resultant thickness values for the respective IMP seams and Al coatings are compiled in Fig. 1. The chosen HDA conditions allow for straightforward comparisons between samples of different Si concentrations and / or IMP thicknesses at similar thickness of the Al coatings. It should be noted that the growth-suppressive effect of Si is complex and does not exhibit linear effects [11,14,21].

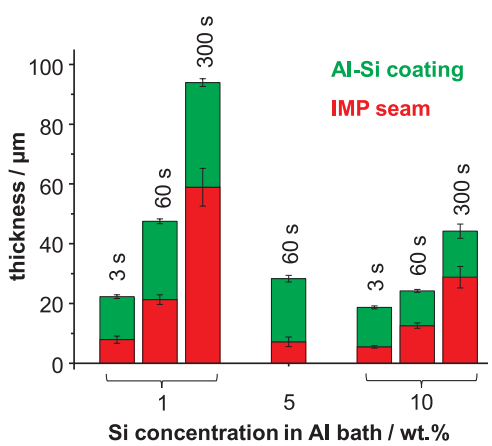

Fig. 1. Thickness of Al-Si coatings and the intermetallic phase seams (IMP) for different bath compositions and dipping times.

Tensile tests at 5 µm s^{-1} initial strain rate were used to elucidate the mechanical performance of the different coatings, i.e. investigating the complex co-deformation phenomena of the strong steel substrate, brittle IMPs and ductile Al. All samples were machined by spark-erosion and taken from the same area of a HDA steel plate, with the tensile axis parallel to the rolling direction. Three setups were used with respective objectives:

(i) Standard tensile testing was performed with a hydraulic testing machine Instron 8511 on specimens according to DIN 50125 E with gauge dimensions of 30 mm length and 8 mm width. The stress and strain levels were approximated by the concepts of engineering stress and strain (i.e. dividing force by initial area and dividing displacement by the initial gauge length, respectively), and the outer surface was observed after the tests by optical microscopy (OM; Keyence digital microscope VHX-5000). All samples showed similar macro-mechanical behaviour, with approximate values of 110 MPa yield stress, 290 MPa ultimate tensile stress, 20% uniform and 40% total elongation. Samples with thicker IMP seams (Fig. 1) generally showed reduced uniform and total elongations.

(ii) Micro-tensile testing was performed with a Kammrath & Weiss setup on specimens with gauge dimensions of 5 mm length and 3 mm width. A speckle pattern applied upon the samples allowed to derive the local strain on the coating through digital image correlation (DIC) measurements using the ARAMIS software package. For investigating the deformation and fracture behaviour of the coating as a function of the local strain, longitudinal sections of the ruptured samples were polished and analysed by OM imaging, as detailed elsewhere [22].

(iii) In order to efficiently investigate the corrosion protection of different coatings affected by varying degrees of mechanical pre-deformation, tensile samples with three gauge sections of identical length (15 mm each) but different width were designed. Based on the data obtained from the standard tensile data, finite element analysis (FEM) for the associated von Mises stress fields was performed using the commercial solver Abaqus/Standard, an isotropic elastic-plastic law and a Young's modulus of 215.623 GPa on a mesh of 33513 linear hexahedral elements of type C3D8R, and 42 linear wedge elements of type C3D6. As shown in Fig. 2, a sample with three separate gauge widths of 15, 9 and 6 mm, respectively, was derived. These dimensions translate to about 100 MPa (i.e. in the elastic region), about 190 MPa (i.e. low plastic strain) and about 290 MPa (i.e. large plastic strains close to necking) at a load of about 1500 N and 6.5 mm crosshead displacement, applied in the hydraulic testing machine Instron 8511 at 5 µm s^{-1}. After the tensile pre-deformation the specimens were subjected to corrosion tests in a salt spray chamber under a constant fog according to the ASTM B117 standard (5 wt% NaCl in water, 35 °C, 100% humidity, up to 300 h). The cut-edges of the samples were painted with an epoxy paint to prevent their corrosion in order to study the effects of the pre-deformed coatings only.

3. Results

3.1. Influence of Si

Three HDA conditions were selected in order to investigate the influence of Si on the mechanical performance, namely Al-1 wt% Si and 3 s dipping time, Al-5 wt% Si for 60 s and Al-10 wt% Si for 3 s, as the resultant IMP seams were of comparable thickness (between 5 and 8 µm; Fig. 1). All three HDA conditions showed similar behaviour under standard tensile loading conditions. As shown on selected samples in Fig. 3, a fishnet-like pattern can be observed on OM images of the coating surface 45° with respect to the tensile direction after about 10%

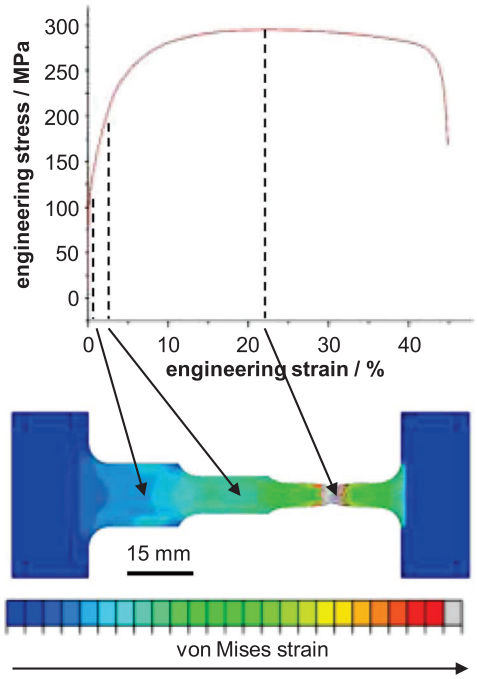

Fig. 2. Example of a stress/strain curve (standard geometry, steel dipped in Al – 10.wt% 10 for 3 s) and FEM calculation result of the three-gauge geometry for corrosion experiments after mechanical pre-deformation.

engineering strain, as well as small cracks in the IMP seam.

Results of more detailed investigations on the damage initiation and progress with increasing tensile strain, performed on micro tensile samples, are compiled in Fig. 4, exemplified on steel dipped for 3 s into Al – 1 wt% Si. Cracks start to form in the IMP seam (about 5–10 per 100 µm interfacial length) perpendicular to the tensile direction at strains below 15% (the limit for reliable strain measurements of the applied DIC setup), covered by a 'bridge' of the Al-based coating. These cracks broaden with increasing strain and horizontal cracks (parallel to the interface with Al-coating and steel substrate) start to appear in the IMP seam. The perpendicular cracks in the IMP widen to about 5–10 µm with increasing strain, and from about 15% elongation the Al coating covering them ruptures (in a ductile manner). Even though the steel is far from mechanical failure at these strain levels (Fig. 2), it is now in direct contact with the surrounding atmosphere and thus potential corrosion, oxidation or decarburisation phenomena (see Section 3.3). No difference could be observed between the three HDA conditions with regards to the basic sequence of damage initiation and progress, as well for the micro-mechanical behaviour of the different IMP phases (all similarly brittle). The critical local strain (i.e. where the coating ruptures and its protection for the steel substrate expires), however, decreases with increasing Si content (from about 20% for Al – 1 wt% Si to 15% or less for 5 and 10 wt% Si), illustrating the Si-induced embrittlement of the Al-coating "bridges" covering the IMP cracks.

3.2. Influence of IMP thickness

The influence of the IMP thickness was evaluated on steel dipped into Al − 10 wt% Si (the most relevant bath composition from an industrial point of view) for 3, 60 and 300 s. These HDA conditions resulted in similar Al-Si coating thicknesses of about 10–15 µm, but varied the thickness of the IMP seam from about 5 to about 30 µm (Fig. 1). Samples with thinner IMP seams, i.e. those dipped for 3 and 60 s, showed a behaviour as those samples described in the previous chapter, i.e. a fishnet-like pattern on the coated surface and small, mostly perpendicular cracks within the IMP seam (Fig. 3). The sample dipped for 300 s, however, behaved differently. As shown in Fig. 5, after about 10% tensile strain (on standard tensile samples) lines perpendicular to the tensile direction appear, and the much thicker IMP seam (> 20 µm) shows less (about 2 cracks per 100 µm interfacial length) but broader perpendicular cracks, as well as horizontal ones. Investigations on micro-tensile specimens revealed a critical local strain (i.e. where the coating fails and the steel is exposed to the atmosphere) of less than 15%. With further increasing nominal strain the coating was observed to flake off the steel substrate to a growing extent, exposing it at mm wide areas. Samples dipped into Al – 1 wt% Si for 60 and 300 s had comparable IMP seam thicknesses (Fig. 1) and behaved similarly than those dipped into Al − 10 wt% Si for 300 s, but less flaking of wide areas of coating due the enhanced ductility of the coating with less Si.

3.3. Corrosion protection after pre-deformation

Salt-spray testing was performed on three-gauge specimens from four different HDA experiments, namely Al – 1 wt% Si dipped for 3 s, Al – 5 wt% Si dipped for 60 s, and Al – 10 wt% Si dipped for 3 and 300 s.

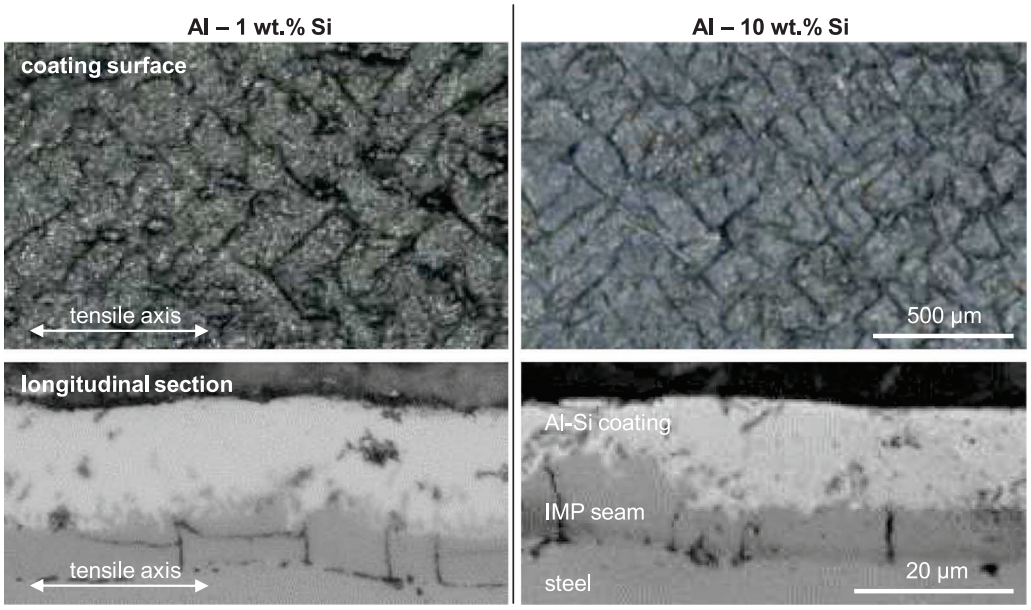

Fig. 3. Optical microscopy characterization results of samples dipped for 3 s and strained to about 10% elongation.

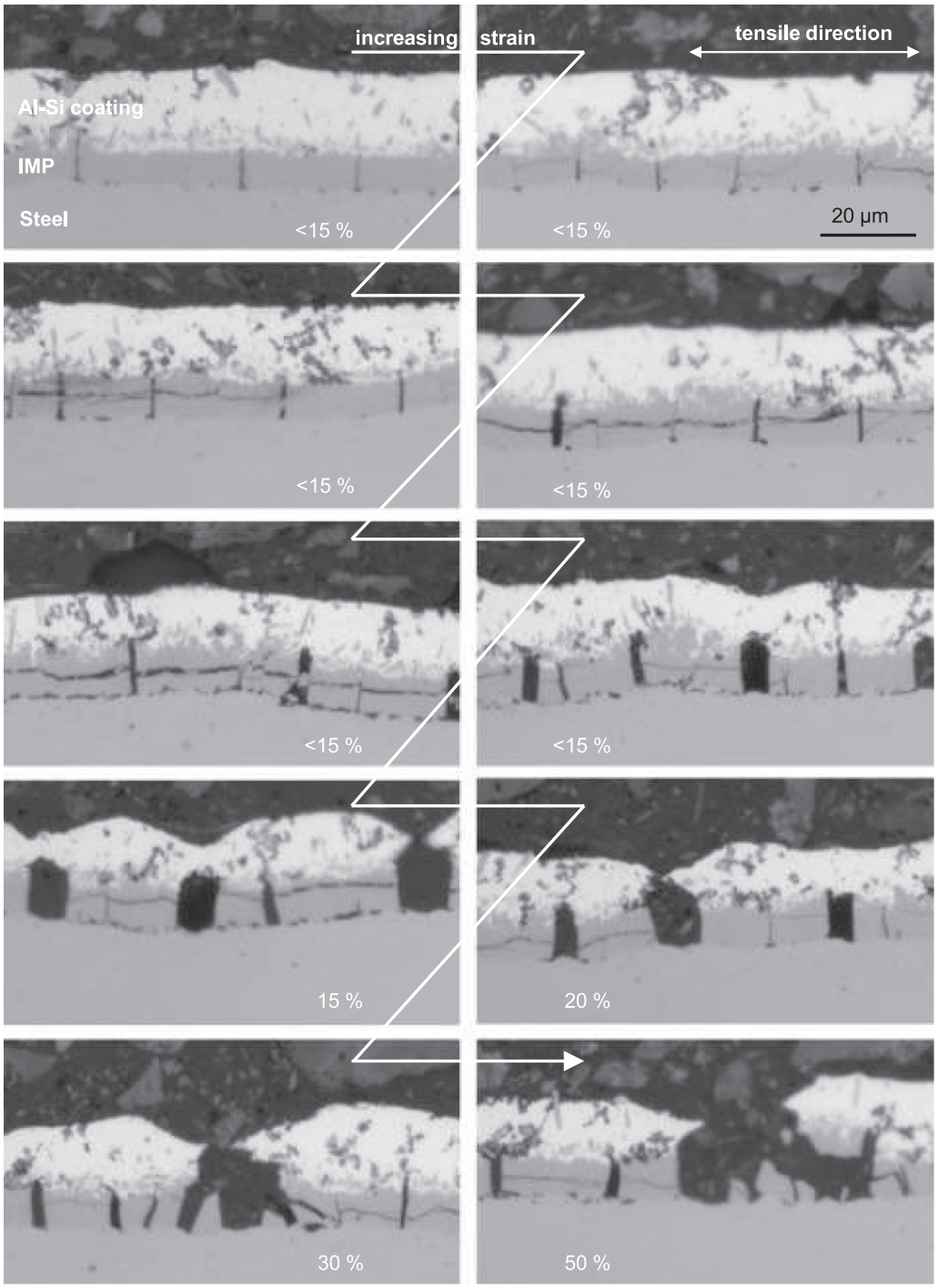

Fig. 4. Damage evolution with increasing local strain (micro-tensile geometry) in longitudinal sections of a sample dipped into Al – 1 wt% Si for 3 s.

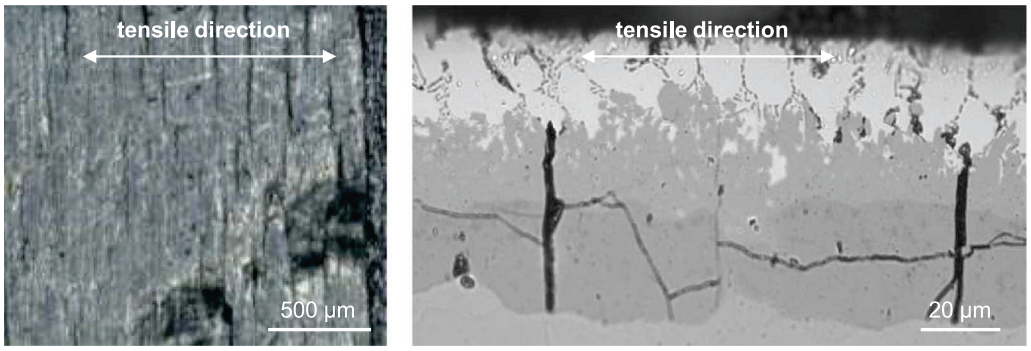

Fig. 5. Optical microscopy characterization results of a sample dipped into Al – 10 wt% Si for 300 s and strained to about 10% elongation (left: coating surface, right: longitudinal section).

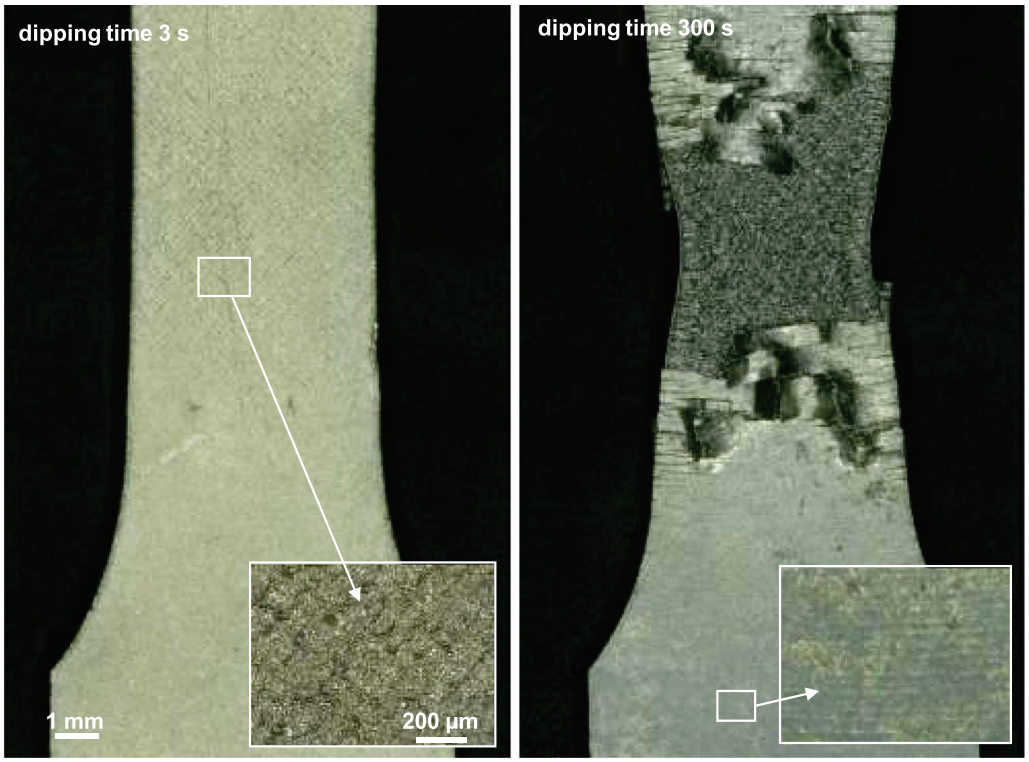

Fig. 6. Surface damage visualized by optical microscopy characterization results of steel samples dipped into Al – 10 wt% Si for different times and corresponding IMP thicknesses. Shown are the thinnest gauge sections of three-gauge samples after mechanical loading prior to the corrosion experiments.

After the mechanical pre-deformation, the specimens from the first three HDA conditions – all with comparatively thin IMP seams – exhibited the previously observed fishnet-like pattern in the medium and thin gauge sections (i.e. those with low and high plastic strain), but no flaking of the coating could be observed (Fig. 6 left) even after severe pre-deformation. Despite the fact that the Al-Si coatings from these three HDA conditions are criss-crossed by crevices leaving the steel substrate exposed, red rust could only be observed at the thinnest gauge section after 300 h exposure within the harsh chloridic environment. The Al-Si coatings are able to protect the steel as its Al_2O_3 surface layer is affected at high chloride environments and leaves Al available to sacrifice itself [23], and rusting appears from the moment at which the coating is consumed.

The much thicker IMP seam of the sample dipped for 300 s, however, caused the coating to flake off in the highest strain gauge section (Fig. 6; right), and started to show red rust already after 2 h of salt-spray testing. The lesser strained gauge sections exhibited lamellar fracture patterns and a similar corrosion behaviour than the samples with thinner IMP seams.

4. Discussion

The Si concentration alone did not have a significant impact on the micromechanical and corresponding corrosion behaviour of the investigated HDA coated steels (Figs. 3 and 6). While Si turned out to slightly embrittle the Al-Si coating, no pronounced influence on the damage evolution was detected (Fig. 4). Significant differences in failure mechanism and critical deformation levels, however, could be observed depending on the thickness of the IMP seam, which was in turn related to the Si content and dipping time (Figs. 1, 5 and 6). The observed different failure patterns in the Al-Si coating (45° fishnet w.r.t. the tensile direction for thinner IMPs, 90° rectangular and larger cracks for thicker IMP seams) and the underlying failure initiation and progressing mechanisms may be rationalised by the schematic sketch shown in Fig. 7. At the top the theoretically expected deformation behaviour of the separate components of an HDA steel sheet (steel substrate, IMP seam and Al-Si coating) under tension are shown. The Young's modulus of the Al based coating can be expected to be only a third of that of DC06 steel (about 70 GPa vs. 210 GPa), while the intermetallic layer has a Young's modulus similar to steel [20]. The consequences are illustrated in the bottom rows of damage evolution schemes. While intermetallic phases are brittle irrespective of their thickness, thicker IMP seams are expected to start cracking at lower strains than thinner ones, with a critical thickness of about 3–10 µm [7]. Thus, the Al coating may already deform plastically before thin IMP seams (obtained after higher Si concentrations and short dipping times) start to crack. As the more ductile Al-Si coating will deform by ductile shear (45° to tensile axis), correspondingly formed shear bands may concentrate stress and thus be the initiation point for IMP cracking, thereby imprinting the deformation pattern of the coating on the IMP seam.

On the other hand, thicker intermetallics (here above about 10 µm) start to crack at lower global strain levels, i.e. before the Al coating could undergo significant (plastic) deformation, and fracture will occur similar to a brittle material under normal tension (i.e. 90° to the tensile direction). As these cracks widen, they concentrate stress at the ductile but soft Al layer, and, at sufficiently high strain levels, cause the remaining coating 'bridges' to fail at the original locations of the first IMP cracks in a lamellar pattern. While these cracks (in a lamellar or angled arrangement) left the steel substrate open for contact with a potentially corrosive environment, they were apparently thin enough to not affect the protective performance of the coatings unduly in the salt-spray experiments conducted in this study (i.e. leaving sufficient amount of Al relative to the crack size to be sacrificially consumed). This should not apply though for oxidation and decarburisation phenomena as during annealing in a hot stamping operation. Our study thus highlights the importance of obtaining regular and thin IMP seams (via appropriate Si additions and short dipping times) in combination with ductile Al-based coatings, as well as the adaption of forming operations and post-processing parameters to maximise the effect of HDA coated steel.

5. Conclusions

In this work, the mechanical performance, fracture and corrosion

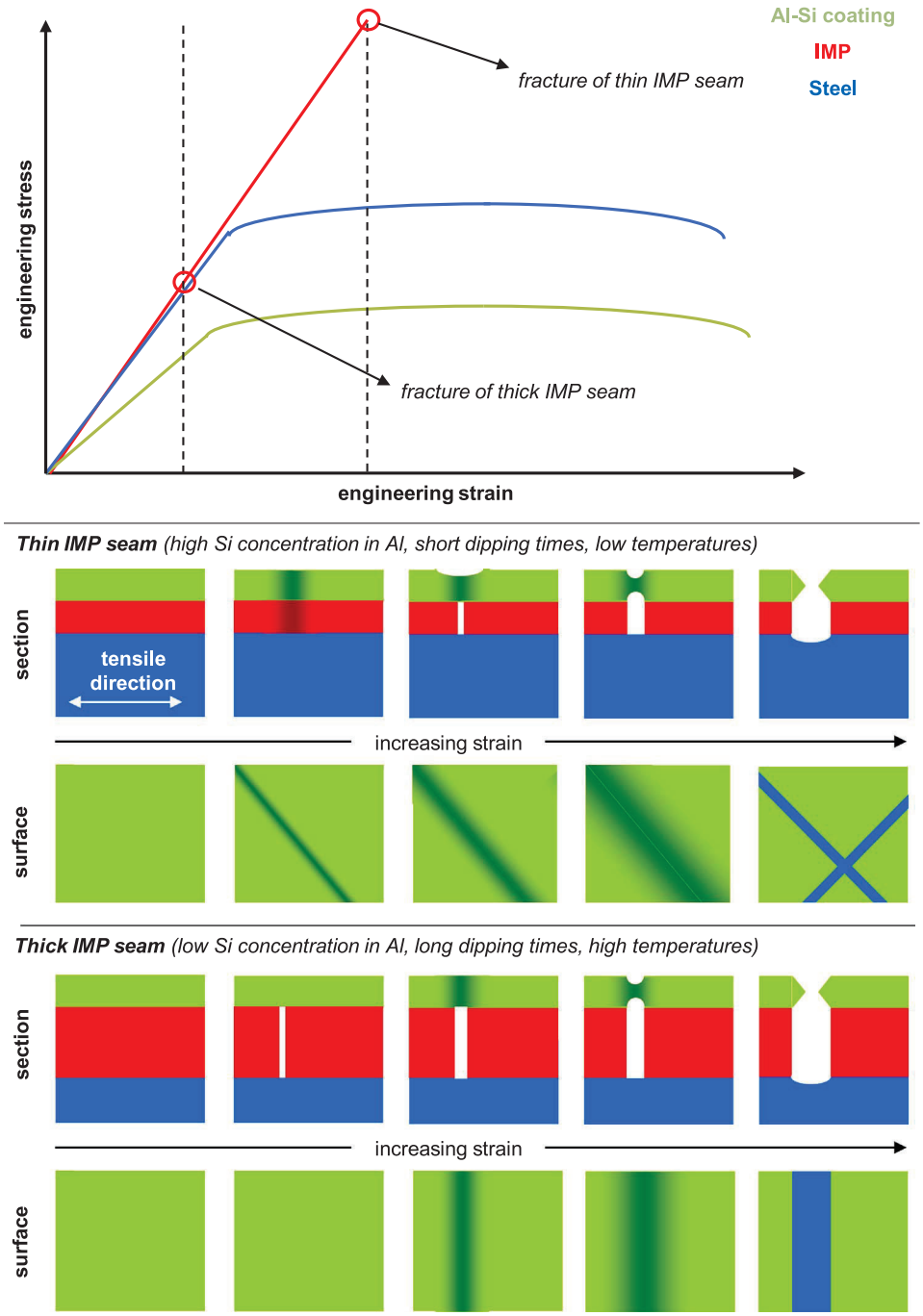

Fig. 7. Sketch of the micromechanical mechanism causing the differing behaviour between hot-dipped aluminized steels with thin and thick intermetallic phase seams (IMP).

behaviour of HDA steels was investigated. The influence of Si and the IMP thickness was examined separately to fully understand their effect on the corresponding corrosion behaviour after mechanical pre-deformation. The addition of Si on itself had no direct influence on the performance of the coating system (i.e. the sum of IMP seam and Al-based coating). Rather the thickness of the IMP seam showed to be the dominant factor independent of its build-up (i.e. with or without Si-induced changes in constituting phases). Thin IMP seams (< about 10 μm) exhibit smaller but more cracks with a fishnet pattern on the outer Al-Si coating, which remains closed and interconnected until a tensile deformation of 15–20%. Thicker IMP seams result in less but broader cracks perpendicular to the tensile direction, giving rise to a lamellar pattern on the Al-Si coating, which already cracks open and uncovers the steel at strains below 10%. In concert with the corrosion tests, our results corroborate that the main target to improve the performance of HDA coated steel is to reduce the IMP thickness, most ideally by combined Si addition and minimized dipping temperatures and times.

References

[1] 〈http://automotive.arcelormittal.com/europe/products/alusi/alusi_general_points/EN〉.
[2] H. Karbasian, A.E. Tekkaya, A review on hot stamping, J. Mater. Process. Technol. 210 (2010) 2103–2118.
[3] P. Hu, L. Ying, Y. Li, Z. Liao, Effect of oxide scale on temperature-dependent interfacial heat transfer in hot stamping process, J. Mater. Process. Technol. 213 (2013) 1475–1483.
[4] G. Zhong-Xiang, W. Kai, Z. Yi-Sheng, Z. Bin, Cracking and interfacial debonding of the Al-Si coating in hotstamping of pre-coated boron steel, Appl. Surf. Sci. 316 (2014) 595–603.
[5] F. Jenner, M.E. Walter, R. Mohan Iyengar, R. Hughes, Evolution of phases, microstructure, and surface roughness during heat treatment of aluminized low carbon

steel, Metall. Mater. Trans. A 41 (2010) 1554–1563.
[6] C. Allely, L. Dosdat, O. Clauzeau, K. Ogle, P. Volovitch, Anticorrosion mechanisms of aluminized steel for hot stamping, Surf. Coat. Technol. 238 (2014) 188–196.
[7] H. Springer, A. Kostka, J.F. dos Santos, D. Raabe, Influence of intermetallic phases and Kirkendall-porosity on the mechanical properties of joints between steel and aluminium alloys, Mater. Sci. Eng.: A 528 (2011).
[8] K. Żaba, Selected problems of formability of aluminised steel plates, Arch. Civil. Mech. Eng. 12 (2012) 163–170.
[9] H. Kawase, A. Takezoe, Peeling of coated metal due to severe pressforming in aluminized steel sheet, Trans. ISIJ 22 (1982) 371–376.
[10] O. Dezellus, B. Digonnet, M. Sacerdote-Peronnet, F. Bosselet, D. Rouby, J.C. Viala, Mechanical testing of steel/aluminium-silicon interfaces by pushout, Int. J. Adhes. Adhes. 27 (2007) 417–421.
[11] M.A. Shady, A.R. El-Sissi, A.M. Attia, On the technological properties of steel strips aluminized in Al-Si baths, J. Mater. Sci. Lett. 15 (1996) 1032–1036.
[12] H. Springer, A. Kostka, E.J. Payton, D. Raabe, A. Kaysser-Pyzalla, G. Eggeler, On the formation and growth of intermetallic phases during interdiffusion between low-carbon steel and aluminum alloys, Acta Mater. 59 (2011) 1586–1600.
[13] M.V. Akdeniz, A.O. Mekhrabov, T. Yilmaz, The role of Si addition on the interfacial interaction in Fe-Al diffusion layer, Scr. Metall. Mater. 31 (12) (1994) 1723–1728.
[14] G. Eggeler, W. Auer, H. Kaesche, On the influence of silicon on the growth of the alloy layer during hot dip aluminizing, J. Mater. Sci. 21 (1986) 3348–3350.
[15] R. Shivpuri, Y.L. Chu, K. Venkatesan, J.R. Conrad, K. Sridharan, M. Shamim, R.P. Fetherston, An evaluation of metallic coatings for erosive wear resistance in die casting applications, Wear 192 (1996) 49–55.
[16] J.E. Nicholls, Hot-dipped aluminium coatings, Anti-Corros. Methods Mater. 11 (1964) 16–21.
[17] X. Zhang, Y. Li, Y. Liu, C. Yang, New evidence for the formation and growth mechanism of the intermetallic phase formed at the Al/Fe interface, J. Mater. Res. 28 (2013) 3279–3287.
[18] V.R. Ryabov, Aluminizing of Steel, Oxonian Press, New Delhi, 1985.
[19] P.R. Goulart, J.E. Spinelli, W.R. Osório, A. Garcia, Mechanical properties as a function of microstructure and solidification thermal variables of Al–Si castings, Mater. Sci. Eng. A 421 (1–2) (2006) 245–253.
[20] H. Springer, Fundamental Research Into the Role of Intermetallic Phases in Joining of Aluminium Alloys to Steel (Ph.D. Thesis), Ruhr Universität Bochum, 2011.
[21] B. Lemmens, H. Springer, I. De Graeve, J. De Strycker, D. Raabe, K. Verbeken, Effect of silicon on the microstructure and growth kinetics of intermetallic phases formed during hot-dip aluminizing of ferritic steel, Surf. Coat. Technol. 15 (2017) 104–109.
[22] H. Springer, C.C. Tasan, D. Raabe, A novel roll bonding methodology for the cross-scale analysis of phase properties and interactions in multiphase structural materials, Int. J. Mater. Res. 106 (2015) 3–14.
[23] Z. Panossian, L. Morcillo, S. Flores, J. Rocha, J.J. Pena, F. Herrera, F. Corvo, M. Sanchez, O.T. Rincon, G. Pridybailo, J. Simancas, Steel cathodic protection afforded by zinc, aluminium and zinc/aluminium alloy coatings in the atmosphere, Surf. Coat. Technol. 190 (2005) 244–248.